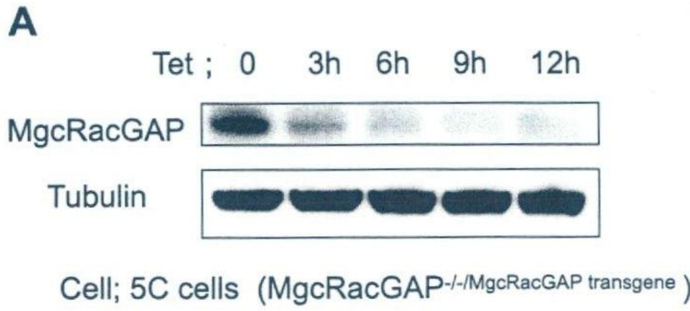

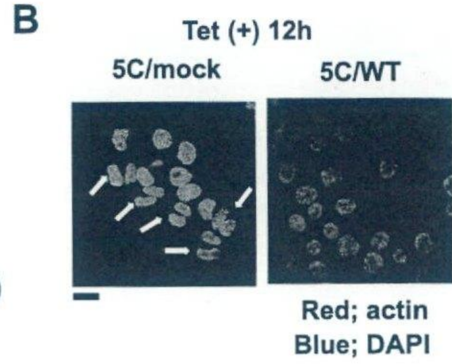

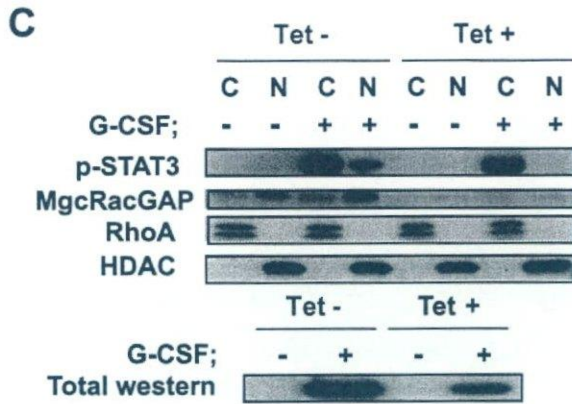

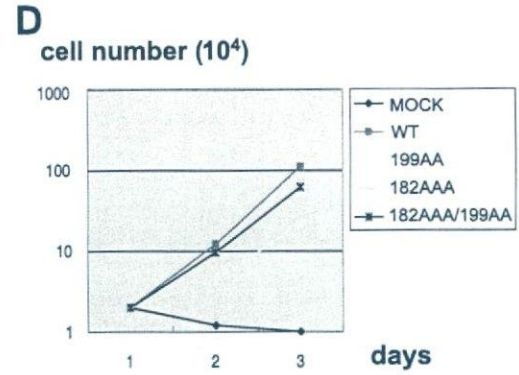

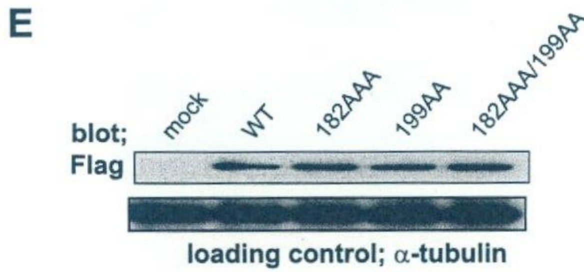

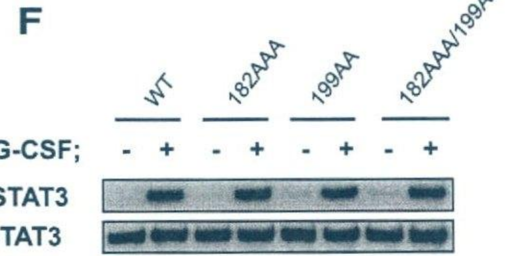

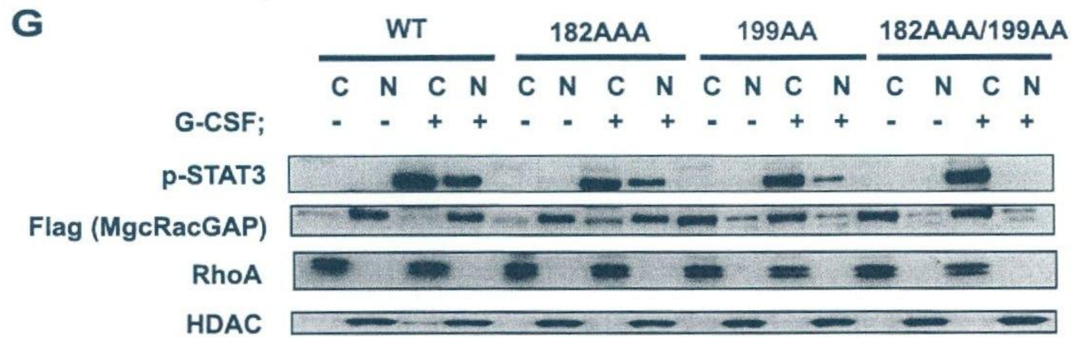

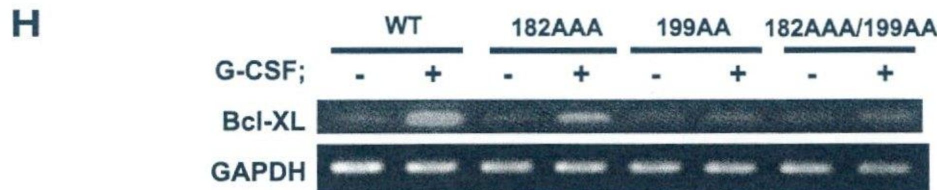

1802

Downloaded from mcb.asm.org at UNIV OF TOKYO on March 29, 2009

scriptional activation of STATs in vivo, we first performed a luciferase assay using 293T cells. The IL-6-induced activation of STAT3 was clearly enhanced by cotransfection with the wild-type MgcRacGAP (~45-fold, compared with mock transfection [~10-fold]). Unexpectedly, cotransfection of the 199AA or 182AAA/199AA mutant modestly inhibited the IL-6-induced transactivation of STAT3 (~25-fold) compared with WT but, rather, enhanced it when compared with mock treatment (data not shown). It is possible that these MgcRacGAP mutants form a heterodimer with endogenous MgcRacGAP and that the heterodimer but not the homodimer of the 199AA or 182AAA/199AA mutant enhanced IL-6-induced transcriptional activation of STAT3. To exclude the effects of endogenous MgcRacGAP, we attempted to establish an MgcRacGAP conditional knockout using DT40 cells. We generated DT40 mutants in which cells with a disrupted MgcRacGAP gene were sustained by expression of the exogenous MgcRacGAP cDNA under the control of a tetracycline-repressible promoter. As shown in Fig. S4A in the supplemental material, an MgcRacGAP-targeting construct was generated such that the 8.0-kb genomic fragment encoding the open reading frame was replaced with one of the two selection cassettes. We transfected the MgcRacGAP-targeting construct containing the histidinol resistance cassette into DT40 cells and isolated MgcRacGAP$^{+/-}$ clones. One MgcRacGAP$^{+/-}$ clone was cotransfected with a chicken MgcRacGAP transgene under the control of a TET-repressible promoter and a TET-repressible transactivator containing a zeocin (ZEO) resistance cassette. We selected ZEO-resistant colonies and identified several clones carrying these constructs integrated at random sites in the genome (MgcRacGAP$^{+/-/\text{MgcRacGAP transgene}}$). Five clones with the MgcRacGAP$^{+/-/\text{MgcRacGAP transgene}}$ genotype were transfected with another MgcRacGAP-targeting construct harboring a puromycin selection marker to disrupt the remaining MgcRacGAP allele. We obtained 24 clones with the MgcRacGAP$^{-/-/\text{MgcRacGAP transgene}}$ genotype, and one clone, 5C, was chosen for further analysis (see Fig. S4B, panels a and b, in the supplemental material). Exogenous MgcRacGAP protein under the control of a TET-repressible promoter in 5C cells was not detected by Western blot analysis with anti-chicken MgcRacGAP Ab at 6 to 12 h after addition of TET, indicating that a TET-repressible promoter of this clone worked successfully and that MgcRacGAP was actively turned over (Fig. 3A). When the expression of the MgcRacGAP transgene was suppressed by adding TET, cell growth of 5C cells was suppressed together with the inhibition of cytokinesis, and the cells formed multinucleated cells, eventually undergoing apoptosis within 48 h (Fig. 3B and data not shown). This phenotype is consistent with the previous result indicating that MgcRacGAP is required for completion of cytokinesis.

The 199AA and 182AAA/199AA mutants inhibited nuclear translocation and transcriptional activation of p-STAT3 in MgcRacGAP knockout cells. To determine if MgcRacGAP is required for the nuclear translocation of p-STAT3 in vivo, we investigated whether depletion of MgcRacGAP affected the subcellular distribution of p-STAT3 after granulocyte colony-stimulating factor (G-CSF) stimulation using the 5C cells. The 5C cells, which had been transiently transfected with a vector carrying a G-CSF receptor, were treated with TET for 4 h and were stimulated with G-CSF (15 min), followed by nuclear-cytosol fractionation analysis. We also confirmed that after treatment with TET for 4 h only a portion of the 5C cells formed multinucleated cells (less than 10%) (data not shown). The nuclear-cytosol fractionation analysis revealed that depletion of MgcRacGAP resulted in a decreased amount of the G-CSF-induced p-STAT3 as well as inhibition of the nuclear accumulation of p-STAT3 (Fig. 3C). These results implied that MgcRacGAP mediates the G-CSF-induced phosphorylation

Downloaded from mcb.asm.org at UNIV OF TOKYO on March 29, 2009

FIG. 3. The NLS of MgcRacGAP is required for the transcriptional activation of p-STAT3 in 5C cells. (A) Suppression of MgcRacGAP by TET in 5C cells. The 5C cells were treated with TET for the time indicated and lysed. Cell lysates were separated on SDS-PAGE and immunoblotted with the anti-chicken MgcRacGAP Ab (upper panel) or anti-α-tubulin Ab (lower panel). (B) Flag-tagged WT MgcRacGAP rescued 5C cells from becoming multinucleated after addition of TET. The 5C cells transduced with mock or Flag-tagged WT were stained with rhodamine-conjugated phalloidin (red) and DAPI (blue) 12 h after the addition of TET and viewed using a FLUOVIEW FV300 confocal microscope (Olympus). Bar, 10 μm. (C) Subcellular localization of p-STAT3 in 5C cells after addition of TET in the absence or presence of G-CSF. Cell fractionation was performed using 5C cells transiently transfected with the expression vector for the G-CSF receptor (G-CSFR). Twenty-four hours after transfection, live cells were isolated using Ficoll-Paque Plus (Amersham) and used for further analysis. Cells were treated or untreated with TET for 4 h and were incubated with 100 ng/ml of G-CSF for 15 min before cell fractionations. Fractionated samples were then subjected to Western blotting with anti-p-STAT3, anti-Flag, anti-RhoA, or anti-HDAC Ab (upper panels). The total amount of p-STAT3 was also examined using whole-cell lysates of 5C cells by Western blotting with anti-p-STAT3 (lower panel). C, cytosol; N, nuclear. (D) Effect of NLS mutants of MgcRacGAP on cell proliferation. Flag-tagged WT or various MgcRacGAP mutants (182AAA, 199AA, and 182AAA/199AA) were transduced into 5C cells by using a retrovirus vector, pMXs-IG. GFP-positive cells were selected by addition of TET. The number of transfectants was counted at the indicated time points after selection. GFP-positive mock-transduced cells, which were analyzed using fluorescence-activated cell sorting, were used as a control. (E) Expression levels of the Flag-tagged WT or mutant MgcRacGAPs in 5C transfectants. Cell lysates from 5C cells expressing mock, WT, or mutant MgcRacGAPs (1×10^7/lane) were examined by Western blotting using the anti-Flag M2 monoclonal antibody (upper panel) or anti-α-tubulin Ab (lower panel). (F) G-CSF-induced phosphorylation of STAT3 in 5C cells expressing Flag-tagged WT or mutant MgcRacGAPs. The 5C cells expressing WT or mutant MgcRacGAPs cotransfected with the expression vector for G-CSFR were stimulated with 100 ng/ml of G-CSF for 15 min in the presence of TET, followed by Western blotting (5×10^6 cells/lane) using the anti-p-STAT3 antibody (upper panel) or anti-STAT3 Ab (lower panel). (G) Subcellular localization of p-STAT3 in 5C cells expressing Flag-tagged WT, 182AAA, 199AA, or 182AAA/199AA with or without G-CSF stimulation in the presence of TET. Cell fractionation was performed using 5C transfectants cotransfected with the expression vector for G-CSFR. Twenty-four hours after transfection, live cells were isolated using Ficoll-Paque Plus (Amersham) and used for further analysis. Cells were incubated with 100 ng/ml of G-CSF for 15 min before cell fractionations. Fractionated samples were then subjected to Western blotting with anti-p-STAT3, anti-Flag, anti-RhoA, or anti-HDAC Ab. (H) G-CSF-induced transcriptional activation of STAT3 was suppressed by depletion of MgcRacGAP. Expression of Bcl-xL or GAPDH mRNA was examined in the 5C transfectants expressing WT, 182AAA, 199AA, or 182AAA/199AA with or without G-CSF stimulation. Cells transiently transfected with G-CSFR were serum starved with or without G-CSF stimulation for 7 h in the presence of TET, followed by semiquantitative RT-PCR.

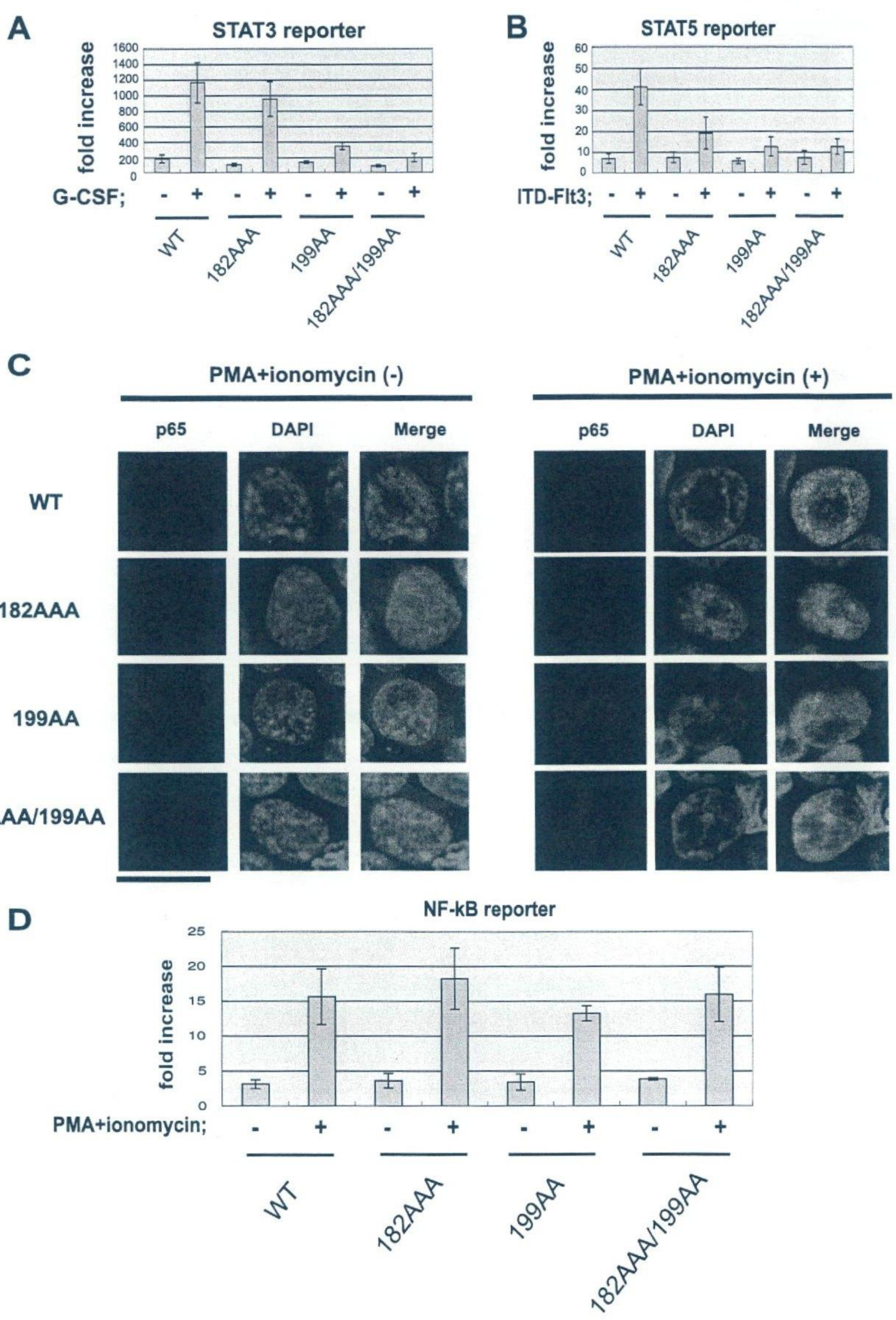

Downloaded from mcb.asm.org at UNIV OF TOKYO on March 29, 2009

and nuclear translocation of p-STAT3. Alternatively, it was possible that depletion of MgcRacGAP indirectly affected activation of STAT3 by disturbing cell cycle machineries. Next, to avoid this possibility, 5C cells were infected with mock or the retrovirus expression vector pMXs-IG carrying WT or the 182AAA, 199AA, or 182AAA/199AA mutant of MgcRacGAP using amphotropic packaging PLAT-A cells (36). The infection efficiencies of these cells were around 10 to 30%, as assessed from the coexpression of GFP using an internal ribosome entry site sequence. After addition of TET, GFP-positive cells grew from the 5C cells transduced with WT or the mutants, while all of the mock-transduced cells became multinucleated, indicating cytokinesis failure, and eventually underwent apoptosis (Fig. 3B and data not shown). These results indicated that the cytokinesis failure of 5C cells after adding TET was prevented by either expression of the WT MgcRacGAP or NLS mutants of MgcRacGAP. All of the 182AAA-, 199AA-, or 182AAA/199AA-expressing cells grew slower than the WT-expressing cells in the presence of TET (Fig. 3D), suggesting that the NLS of MgcRacGAP plays some role in enhancing cell growth but is dispensable for completion of cytokinesis in 5C cells. Expression levels of WT MgcRacGAP or 182AAA, 199AA, or 182AAA/199AA mutant were comparable as assessed in Western blot analyses (Fig. 3E). We next investigated whether disruption of the NLS of MgcRacGAP affected the subcellular distribution of endogenous p-STAT3 after G-CSF stimulation by using the 5C transfectants in the presence of TET. The 5C cells expressing WT MgcRacGAP or the 199AA or 182AAA/199AA mutant, which had been transiently transfected with a vector carrying the G-CSF receptor, were stimulated with G-CSF (15 min). The amounts of G-CSF-induced p-STAT3 in 5C transfectants expressing the WT and those expressing the NLS-lacking mutants were found to be comparable (Fig. 3F). Interestingly, the nuclear-cytosol fractionation analysis revealed that the 199AA- or 182AAA/199AA-MgcRacGAP hardly entered the nucleus, and the G-CSF-induced nuclear accumulation of p-STAT3 was strongly inhibited in 199AA- or 182AAA/199AA-expressing cells compared with those in the 182AAA- and WT-expressing cells (Fig. 3G). We also performed a semiquantitative RT-PCR analysis to test if induction of Bcl-xL mRNA (one of the target genes of STAT3) was affected in the transfectants expressing the NLS-lacking mutants of MgcRacGAP after the G-CSF stimulation, and we found that induction of Bcl-xL mRNA in response to G-CSF stimulation was severely impaired in the transfectants expressing 199AA or 182AAA/199AA (Fig. 3H).

The 199AA and 182AAA/199AA mutants specifically blocked transcriptional activation of p-STATs in MgcRacGAP knockout cells. Next, we performed a luciferase assay using the 5C transfectants cultured in the presence of TET. Transcriptional activities of STAT3 in response to G-CSF stimulation were strongly inhibited in the 199AA- or 182AAA/199AA-expressing 5C cells compared to those in the WT-expressing cells (Fig. 4A). We obtained similar results for STAT5; transcriptional activation of STAT5 induced by ITD-Flt3 was profoundly inhibited in the 199AA- or 182AAA/199AA-expressing 5C cells compared to those in the WT-expressing cells (Fig. 4B). However, NF-κB p65, whose NLS is unmasked by IκBα degradation and binds importins α3 and α4 (8, 23), entered the nucleus after stimulation even in the 199AA- or 182AAA/199AA-expressing cells (Fig. 4C). In addition, transcriptional activities of NF-κB in response to stimulation with PMA/ionomycin were not affected in the 199AA- or 182AAA/199AA-expressing 5C cells compared to those in the WT-expressing cells (Fig. 4D), indicating that MgcRacGAP does not work as a general nuclear chaperone.

The series of STAT3 mutants harboring deletions in the two strands (βa′ and βb) of the β-barrel lost transcriptional activities, while the mutants harboring deletions in the region following the strand βb (βb-βc loop) showed constitutively active phenotypes. We previously found that STAT3 and STAT5 directly bound MgcRacGAP through aa 338 to 362 and aa 341 to 365 in their DNA binding domain, respectively (termed DB2-STAT3 and DB2-STAT5) and that the STAT3 and STAT5A mutants lacking DB2 (STAT3-dDB2 and STAT5A-dDB2) lost not only the capability for binding to MgcRacGAP but also their transcriptional activities (17). The DB2 region is well-conserved among STAT family proteins. In this study, we produced a series of deletion mutants lacking a three-amino-acid stretch in the DB2-STAT3 region (STAT3-dD1 to -8) and in the next six amino acids (STAT3-dD9 and -10) (Fig. 5A). Tyrosine phosphorylation of STAT3-dDB2, -dD1, -dD3, -dD4, or -dD5 in response to IL-6 stimulation was diminished, whereas tyrosine phosphorylation of STAT3-dD2 was prominent even in the absence of IL-6 (Fig. 5C, middle panel). In addition, association of STAT3-dDB2, -dD1, -dD3, -dD4, or -dD5 with MgcRacGAP was not detected, while binding of STAT3-dD2 with MgcRacGAP increased compared

FIG. 4. The NLS of MgcRacGAP is not required for activation of NF-κB p65 in 5C cells. (A) The NLS of MgcRacGAP was required for transcriptional activities of STAT3. Luciferase activities were examined in the lysates of 5C transfectants cotransfected with the STAT3 reporter plasmid, internal control plasmid, expression vector for the G-CSF receptor, or expression vector for the WT-STAT3 (pME/STAT3). After the transfection, cells were incubated with 100 ng/ml of G-CSF for the last 12 h before cell lysates were prepared. Cell lysates were then subjected to a dual luciferase reporter system (Promega). The results shown are the averages ± standard deviations of three independent experiments. (B) The NLS of MgcRacGAP was required for transcriptional activities of STAT5. This experiment was identical to that in panel A, except that 5C transfectants were cotransfected with the STAT5 reporter plasmid, internal control plasmid, or expression vector for the WT STAT5A (pME/STAT5A), together with either the mock or expression vector for ITD-Flt3. (C) The NLS of MgcRacGAP is dispensable for the nuclear translocation of NF-κB p65 in 5C cells. Immunostaining was performed using the 5C transfectants cotransfected with the expression vector for NF-κB p65. After the transfection, cells were serum starved for 3 h, incubated with 30 nM PMA and 1 μM ionomycin for 30 min, and stained with the anti-NF-κB p65 and DAPI. Cells were viewed with a FLUOVIEW FV300 confocal microscope (Olympus). Bar, 10 μm. (D) The NLS of MgcRacGAP was dispensable for transcriptional activities of NF-κB. Luciferase activities were examined in the lysates of 5C transfectants cotransfected with the NF-κB reporter plasmid (k9) carrying a firefly luciferase gene driven by the IL-6 promoter together with the internal control plasmid. After the transfection, cells were incubated with 30 nM PMA and 1 μM ionomycin for 12 h before cell lysates were prepared. Cell lysates were then subjected to a dual luciferase reporter system (Promega). The results shown are the averages ± standard deviations of three independent experiments.

Downloaded from mcb.asm.org at UNIV OF TOKYO on March 29, 2009

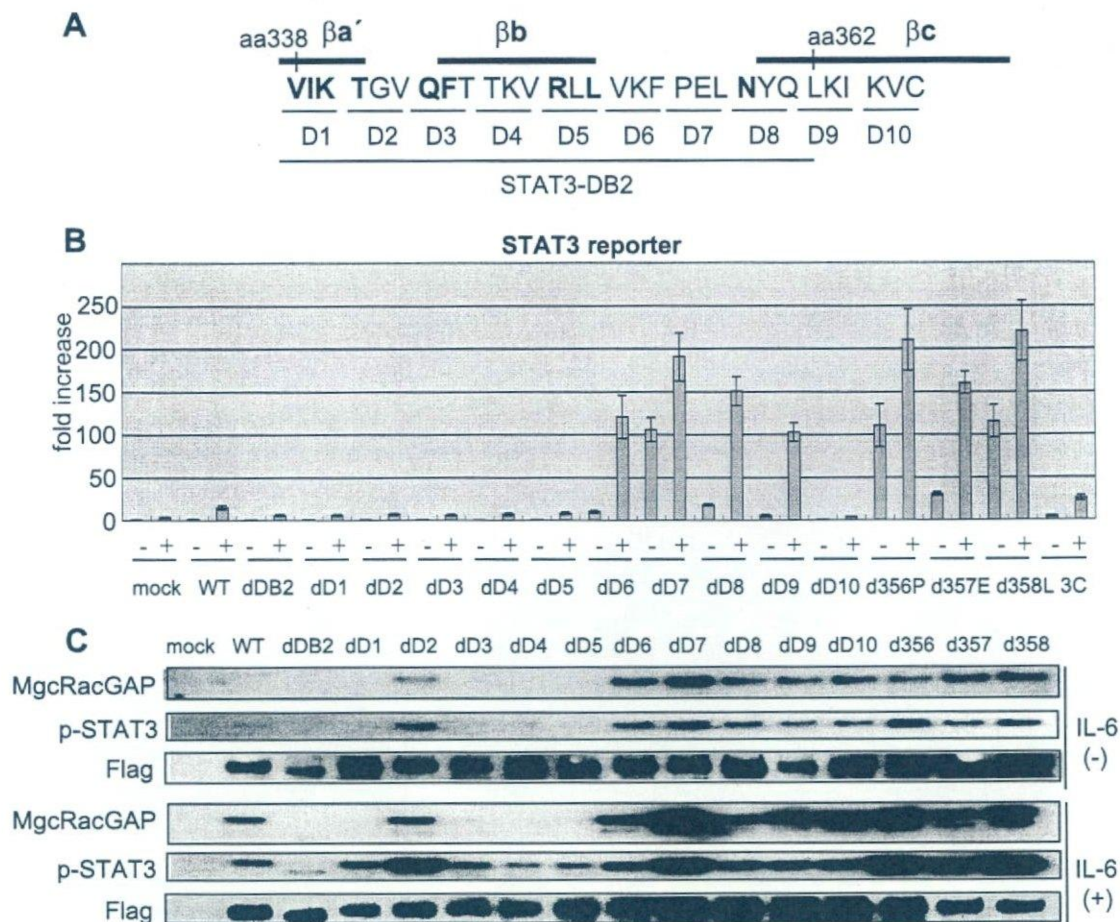

FIG. 5. Correlation between binding abilities of STAT3 to MgcRacGAP and activities of STAT3. (A) Schematic diagrams showing a series of the deletion sites of STAT3 mutants. (B) Transcriptional activities of STAT3 mutants harboring deletions in DB2. Luciferase activity was examined as described in Materials and Methods. As a control, a reported constitutively active mutant of STAT3C was used. The results shown are the averages ± standard deviations of three independent experiments. (C) MgcRacGAP binding abilities of the STAT3 mutants. Tyrosine phosphorylation and binding affinity to MgcRacGAP of Flag-tagged deletion mutants of DB2-STAT3 in the absence or presence of IL-6-stimulation were determined by immunoprecipitation using the anti-Flag Ab followed by Western blotting with the anti-p-STAT3, anti-MgcRacGAP, or anti-Flag Ab. Expression, tyrosine phosphorylation, and interaction with MgcRacGAP of the Flag-tagged deletion mutants of DB2-STAT3 (lower panel, middle panel, and upper panel, respectively) were examined by immunoprecipitation using 293T cells transfected with each of the STAT3 mutants in the absence (upper three panels) or presence (lower three panels) of IL-6-stimulation for 30 min.

Downloaded from mcb.asm.org at UNIV OF TOKYO on March 29, 2009

with that of WT in the absence or presence of IL-6 stimulation (Fig. 5C, upper panels). Nonetheless, the mutants lacking D1 to -5 (STAT3-dD1 to -5), including STAT3-dD2, did not show detectable transcriptional activities in response to IL-6 stimulation (Fig. 5B). Surprisingly, STAT3-dD6 to -9 mutants exerted considerable transcriptional activities even without cytokine stimulation, and this was further enhanced by IL-6 stimulation (Fig. 5B). These mutants were constitutively tyrosine phosphorylated, and their tyrosine phosphorylation was augmented after IL-6 stimulation (Fig. 5C). STAT3-dD10 was constitutively tyrosine phosphorylated but did not show detectable transcriptional activities, as was the case for STAT3-dD2. We next examined whether these STAT3 mutants harbored the DNA binding activities in an electrophoretic mobility shift assay using unstimulated 293T cells and found that unlike the other constitutively tyrosine-phosphorylated STAT3 mutants, STAT3-dD2 and STAT3-dD10 lost their DNA binding affinities (data not shown). Notably, STAT3-dD7 showed the strongest transcriptional activities in the absence of cytokine stimulation among the STAT3-dD1 to -10 mutants, and its transcriptional activities in the absence of cytokine stimulation were much stronger than that of the WT after IL-6 stimulation (Fig. 5B). We next produced a series of mutants lacking each single amino acid of the three amino acids in the region of D7 (STAT3-d356P, -d357E, and -d358L). Interestingly, STAT3-d356P, -d357E, and -d358L, which strongly bound MgcRacGAP, displayed the constitutive activities in the absence of IL-6 stimulation (Fig. 5B and C). STAT3-d356P and STAT3-d358L exerted the strongest transcriptional activity among these mutants and a reported constitutively active mutant of STAT3C (3). These results suggest that the two strands (βa′ and βb) in DB2 are required for the IL-6-induced tyrosine phosphorylation of STAT3 that mediates the interaction with MgcRacGAP, whereas the deletion mutants in the C terminus

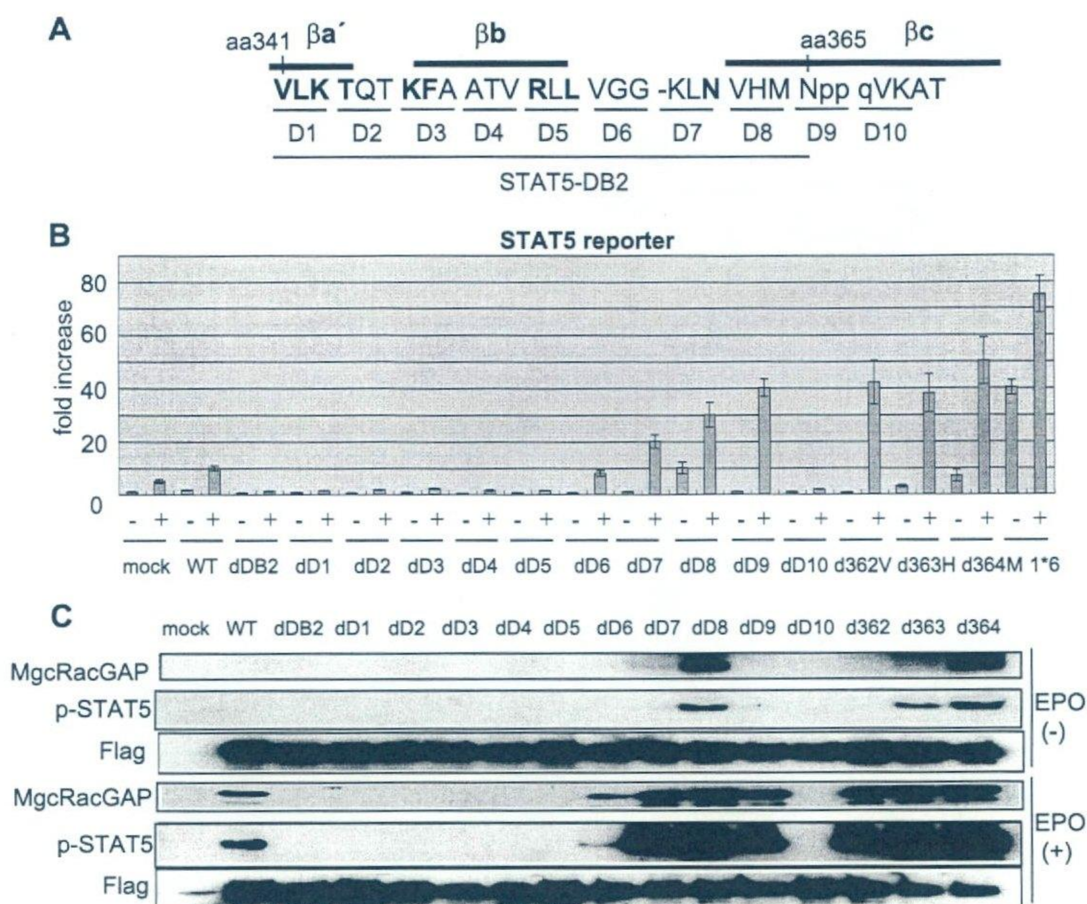

FIG. 6. The series of deletion mutants of STAT5A in DB2 showed similar phenotypes to those of STAT3. (A) Schematic diagrams showing a series of the deletion mutants of STAT5A. (B) The mutants lacking D1 to -5 and D10 (STAT5A-dD1 to -5 and STAT5A-dD10) as well as the STAT5A-dDB2 lacked their transcriptional activities even under EPO stimulation. Luciferase activity was examined in the lysates of unstimulated or EPO (18 ng/ml)-stimulated 293T cells cotransfected with the expression vector for the EPO receptor (EPOR) and STAT5 reporter plasmid together with internal control reporter plasmids and either the mock vector (pME), the expression vector for the Flag-tagged WT STAT5A, or a series of STAT5A mutants harboring deletions in DB2. As a control, the constitutively active STAT5A1*6 mutant was used. The results shown are the averages ± standard deviations of three independent experiments. (C) The mutants of STAT5A harboring deletions in the two strands (βaprime] and βb) lost binding affinities to MgcRacGAP or did not undergo tyrosine phosphorylation, while the mutants harboring deletions in the region following the strand βb showed enhanced binding affinities to MgcRacGAP and underwent enhanced tyrosine phosphorylation. Expression, tyrosine phosphorylation, and interaction with MgcRacGAP of the Flag-tagged deletion mutants of DB2-STAT5A (lower panel, middle panel, and upper panel, respectively) were examined by immunoprecipitation using 293T cells cotransfected with EPOR and each of the STAT5A mutants in the absence (upper three panels) or presence (lower three panels) of EPO stimulation for 30 min.

of DB2 following the strand βb (βb-βc loop) tend to become constitutively active with enhanced binding to MgcRacGAP.

We also produced a series of STAT5A mutants lacking a three-amino-acid stretch in the region corresponding to DB2-STAT3 (STAT5A-dD1 to -8) and in the next six amino acids (STAT5A-dD9 and -10) (Fig. 6A). We found that the series of deletion mutants of STAT5A in DB2 showed phenotypes similar to those of STAT3 mutants (Fig. 6B and C); STAT5A mutants harboring deletions in the two strands (βa′ and βb) of the β-barrel (STAT5A-dD1 to -5) were not tyrosine phosphorylated by EPO stimulation and lost transcriptional activity, while the mutants harboring deletions in the region following the strand βb (STAT5A-dD7 to -9) showed gain-of-function phenotypes. STAT5A-dD8, -d363H, and -d364M also showed constitutively active phenotypes (Fig. 6B and C), although the transcriptional activities of these mutants without stimulation were weaker than that of another constitutively active mutant, STAT5A1*6 (37). Constitutive activities of STAT5A mutants were well-correlated with constitutive binding to MgcRacGAP. Association between the constitutively active STAT5A mutants and MgcRacGAP was stronger than that of the WT and MgcRacGAP in the absence of EPO stimulation (Fig. 6C). Thus, the molecular basis of the STAT-MgcRacGAP interaction is well-conserved between STAT3 and STAT5A.

The constitutively active mutant STAT3-d358L promoted cell proliferation of a mutant cell line derived from BaF-BO3 cells. We next examined whether STAT3-d358L was biologically functional, showing physiological roles of STAT3 activation. It has been reported that BaF-BO3 cells expressing a G-CSF receptor mutant (G133 cells) are able to proliferate in

Downloaded from mcb.asm.org at UNIV OF TOKYO on March 29, 2009

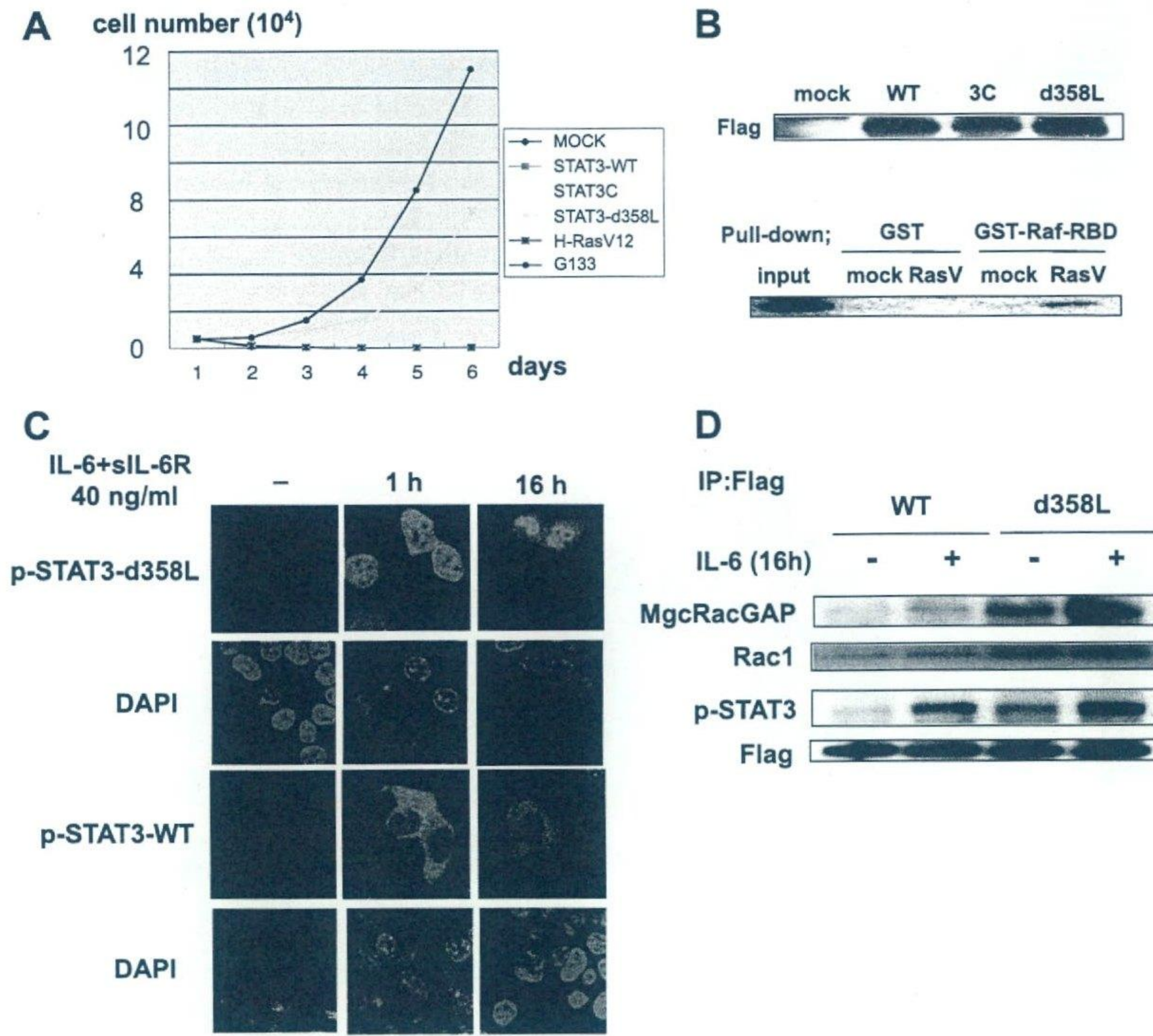

FIG. 7. A constitutively active STAT3 mutant, STAT3-d358L, preferentially bound MgcRacGAP and Rac1 and accumulated to the nucleus. (A) STAT3-d358L supports proliferation of BaF-BO3-G133F3 cells in the presence of G-CSF. BaF-BO3-G133F3 cells expressing mock vector or the Flag-tagged WT STAT3, STAT3C, STAT3-d358L, or H-RasV12 were cultured in the presence of G-CSF, and the cell numbers were determined at the indicated times. BaF-BO3-G133 cells were used as a control. (B) Similar expression levels of WT STAT3, STAT3C, and STAT3-d358L were confirmed by Western blotting with the anti-Flag Ab (upper panel). The expression and activation of H-RasV12 were examined by Western blotting with the anti-Flag Ab (lower panel; input lane) and by pull-down assay using GST–Raf-RBD (lower panel; other lanes), respectively. (C) The STAT3-d358L mutant preferentially accumulated to the nucleus. 293T cells were transfected with pME/STAT3-d358L-Flag (upper panels) or pME/WT-STAT3-Flag (lower panels). After 24 h, the cells were stimulated with IL-6 for the time indicated and fixed, followed by immunostaining with the anti-p-STAT3 or anti-Flag Ab (data not shown). Bar, 10 μm. (D) STAT3-d358L constitutively bound MgcRacGAP and Rac1. Interaction of MgcRacGAP or Rac1 with WT STAT3 or STAT3-d358L was examined by coimmunoprecipitation (IP) using 293T cells transfected with either WT-STAT3 or STAT3-d358L in the absence or presence of IL-6 stimulation (upper two panels). Expression and tyrosine phosphorylation of Flag-tagged WT STAT3 or STAT3-d358L (lower two panels) were also examined.

response to G-CSF stimulation via activating SHP-2/mitogen-activated protein kinase and JAK/STAT3 pathways (10). This mutant receptor, G133, is a chimeric receptor composed of the extracellular domain of the G-CSF receptor and the transmembrane and cytoplasmic domains of gp130 truncated 133 amino acids from the transmembrane domain. Mutation of the tyrosine residue in the YXXQ motif within G133 (G133F3) abolished STAT3 activation and, thus, cell proliferation driven by G-CSF (10). G133F3 cells were transduced with the pMX-puro vector carrying the WT STAT3, STAT3C, STAT3-d358L, a constitutively active mutant H-Ras (H-RasV12), or the expression vector alone (mock). Expression levels of WT STAT3, STAT3C, and STAT3-d358L were similar as judged by Western blotting (Fig. 7B, upper panel). The expression and activation of H-RasV12 were confirmed by Western blotting (Fig. 7B, lower panel, input lane) and by a pull-down assay using GST–Raf-RBD (Fig. 7B, lower panel, other lanes), respectively. As shown in Fig. 7A, STAT3-d358L but neither WT, STAT3C, H-RasV12, nor mock treatment promoted cell proliferation of G133F3 cells under G-CSF stimulation, suggesting

Downloaded from mcb.asm.org at UNIV OF TOKYO on March 29, 2009

that the STAT3-d358L mutant is biologically functional and could be a useful tool to study the physiological roles of STAT3 activation. This result also indicates that STAT3-d358L is stronger than STAT3C in inducing STAT3-dependent cell growth, which is consistent with their transcriptional activities (Fig. 5B).

Interestingly, the tyrosine-phosphorylated form of STAT3-d358L accumulated to the nucleus after IL-6 stimulation more evidently than that of the WT STAT3 (Fig. 7C). Importantly, the STAT3-d358L bound MgcRacGAP and Rac1 more strongly than the WT in the absence or presence of IL-6 stimulation (Fig. 7D). Although most of the phosphorylated form of overexpressed WT STAT3 remained in the cytoplasm (Fig. 7C), this was probably because p-STAT3 requires MgcRacGAP/Rac1 as cofactors to enter the nucleus and these cofactors are limiting the nuclear translocation of p-STAT3. Taken together, our results strongly indicate that the interaction of STATs with MgcRacGAP accompanied by GTP-bound Rac1 plays critical roles in regulating STAT functions through facilitating both tyrosine phosphorylation of STATs and nuclear translocation of p-STATs.

DISCUSSION

We originally identified MgcRacGAP in a search for key molecules that are involved in the IL-6-induced macrophage differentiation of M1 cells (18) and found that MgcRacGAP and Rac1 form a ternary complex with STAT3 and are required for STAT3 activation (43). We also reported that MgcRacGAP localizes to the midbody of dividing cells and plays a crucial role in the completion of cytokinesis, thus playing a distinct role in the mitotic phase (12, 33). We recently found that GTP-bound Rac1 and MgcRacGAP are required for nuclear translocation of p-STATs via the importin pathway in an in vitro nuclear transport assay (17). In this paper, to identify the molecular mechanisms of how GTP-bound Rac1 and MgcRacGAP facilitate complex formation of p-STATs with importin αs, we used MgcRacGAP conditional knockout chicken DT40 cells (5C cells) as well as a nuclear transport assay and demonstrated that the NLS of MgcRacGAP plays a critical role in the nuclear translocation of p-STAT3/5. Although the biological functions of STAT3 and STAT5 are not identical, we demonstrated that nuclear import of p-STAT3 and p-STAT5 was mediated by MgcRaGAP and its NLS, and the molecular mechanisms are common.

Liu et al. (25) reported that constitutive nuclear import of STAT3 monomer is independent of tyrosine phosphorylation and is mediated by importin α3. They found that a deletion mutant of STAT3 (d150-163) (aa 150 to 162; DVRKRVQDL EQKM) did not enter the nucleus. However, the substitution mutant of the basic amino acid cluster in this sequence did not hamper nuclear accumulation. Based on these results, they reasoned that aa 150 to 162 play a role in a conformational structure that is required for nuclear import (25). Similarly, Zeng et al. reported that aa 138 to 165 of STAT5B are required for constitutive nuclear import of STAT5B monomer but that this region does not harbor polybasic amino acids (49). Thus, it was not clear whether STAT3 and STAT5 harbor a functional NLS or whether dimer formation creates a polybasic NLS of STAT3 and STAT5. We here propose that MgcRacGAP accompanied by GTP-bound Rac1 functions as an NLS-containing nuclear chaperone toward p-STATs (Fig. 2B and C). Interestingly, Rac1 was reported to play a role in the nuclear import of SmgGDS and p120 catenin (22), members of the importin α-like armadillo family of proteins (4, 38). The C-terminal region of Rac1, but not Rac2 or Rac3, contains a polybasic region, which may function as an NLS. However, Lanning et al. (22) also suggested that the interaction of Rac1 with its GTP exchange factor SmgGDS was qualitatively different from that of NLS-containing molecules with importin αs. Consistent with this, we failed to detect direct interactions of GTP-bound Rac1 with importin αs in either the in vitro binding assay or yeast two-hybrid assay (data not shown). Therefore, it is unlikely that GTP-bound Rac1 serves directly as an NLS-containing chaperone of p-STATs. The results shown in Fig. 2C strongly indicate that GTP-bound Rac1 activates the NLS MgcRacGAP associating with p-STATs; however, the precise molecular mechanism for the requirement of Rac1 remains to be clarified by structural analysis.

The present results demonstrate that the bipartite NLS (182KRR/199KK) of MgcRacGAP is essential for the nuclear transport and the transcriptional activation of p-STATs in living cells (Fig. 3G and H and 4A). The results of the nuclear-cytosol fractionation analysis using the 5C cells expressing 199AA and 182AAA/199AA (Fig. 3G) also suggested that the preferential nuclear localization of MgcRacGAP is mediated by the importin pathway in living cells. However, in the nuclear transport assay using semi-intact cells and purified proteins, nuclear translocation of MgcRacGAP was not achieved by the addition of importin α/β pathway proteins alone and, interestingly, further addition of p-STATs and GTP-bound Rac1 was required for nuclear translocation of MgcRacGAP (see Fig. S3A and B in the supplemental material). This raised a question of why overexpressed MgcRacGAP predominantly accumulated to the nucleus in HeLa cells, where STATs were not extensively activated. In addition, purified MgcRacGAP pulled down importin αs from the HeLa cell lysate (see Fig. S1B in the supplemental material), while it did not bind purified importin αs in the in vitro binding assay (Fig. 2C and data not shown). These results suggest that the NLS of MgcRacGAP can be activated by other cargo proteins as well as by p-STAT and GTP-bound Rac1. Thus, MgcRacGAP may function as a nuclear chaperone for not only p-STATs but also another nuclear protein(s).

The conditional knockout of MgcRacGAP in 5C cells decreased the G-CSF-induced tyrosine phosphorylation of STAT3 (Fig. 3C), and small interfering RNA-mediated MgcRacGAP knockdown in Ba/F3 cells also reduced tyrosine phosphorylation of STAT5 (17). These results implied that MgcRacGAP functions as an upstream regulator of STAT activation as well. In relation to this, STAT mutants harboring deletions in the βb-βc loop showed enhanced interaction with MgcRacGAP and became constitutively active (Fig. 5 and 6). It should be noted that the extent of tyrosine phosphorylation of STAT3-d358L without stimulation was weaker than that of WT 16 h after IL-6 stimulation (Fig. 7D), although the association of STAT3-d358L with MgcRacGAP/Rac1 was stronger than that of WT under the same conditions (Fig. 5C and 7D). These results indicate that the stronger association of the constitutively active STAT mutants with MgcRacGAP was not a

Downloaded from mcb.asm.org at UNIV OF TOKYO on March 29, 2009

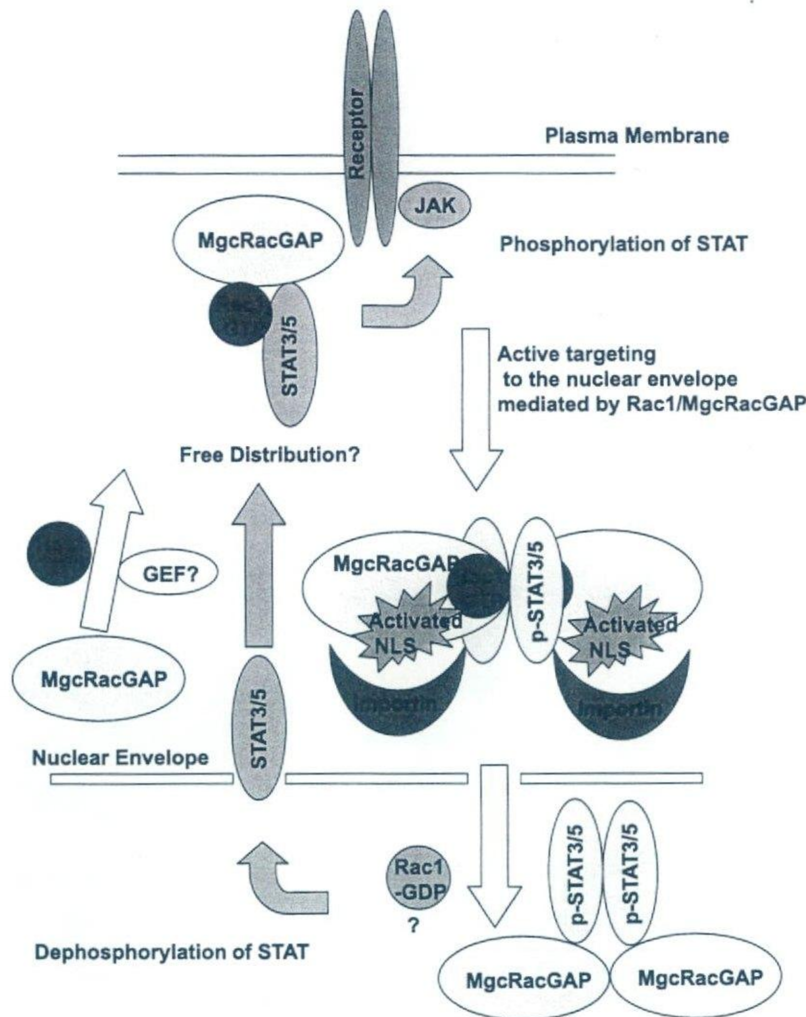

FIG. 8. A current model of nuclear import of p-STATs and a working hypothesis for membrane targeting and phosphorylation of STATs. In the present work, we demonstrated that the NLS of MgcRacGAP accompanied by GTP-bound Rac1 is essential for nuclear translocation of p-STATs via importin α/β. We also propose that binding of MgcRacGAP to STATs is required for their tyrosine phosphorylation after cytokine stimulation. Interestingly, the mutants that preferentially bind MgcRacGAP become constitutively active. Altogether, we conclude that MgcRac-GAP critically functions both as a mediator of STAT's tyrosine phosphorylation and as an NLS-containing nuclear chaperone of p-STATs.

Downloaded from mcb.asm.org at UNIV OF TOKYO on March 29, 2009

secondary result following the enhanced tyrosine phosphorylation of these mutants, and they imply a positive role for MgcRacGAP in facilitating STAT activation. In this context, it is interesting to note that V12Rac1 induced translocation of MgcRacGAP to the plasma membrane (see Fig. S5 in the supplemental material) and that MgcRacGAP bound JAK2 (17). In addition, the interaction of the STAT3-Y704F mutant, which does not undergo tyrosine phosphorylation, with MgcRacGAP was enhanced by IL-6 stimulation, similar to that of the WT STAT3 (data not shown). This indicates that the IL-6-induced MgcRacGAP interaction with STATs does not require tyrosine phosphorylation of STATs and occurs before their tyrosine phosphorylation. Based on these observations, we propose a model of STAT nucleo-cytoplasmic shuttling regulated by Rac1/MgcRacGAP (Fig. 8).

One important finding of the present paper is that the abilities of STAT mutants to bind MgcRacGAP correlated well with the activation of STATs (Fig. 5 and 6). To reveal the molecular mechanisms of MgcRacGAP-mediated regulation of STAT phosphorylation, we conducted an in vitro kinase reaction of purified STAT5 using purified JAK2 in the presence or absence of Rac1 and MgcRacGAP. However, STAT phosphorylation was not enhanced by the addition of Rac1/MgcRacGAP in this mixture (data not shown). Based on the result that MgcRacGAP binds JAK2, we speculate that MgcRacGAP regulates STAT phosphorylation by conveying STAT proteins to JAK2 or by serving as a scaffold for the interaction of JAK2 and STAT.

We also observed that STAT3-d358L bound MgcRacGAP more strongly than WT STAT3 did in yeast (data not shown). In the crystal structure of tyrosine-phosphorylated STAT3β (2) (PDB ID 1BG1), the MgcRacGAP binding DB2 region includes the C terminus of the βa′ strand, the DNA-bound βa′-βb loop, the βb strand, the βb-βc loop, and the N terminus

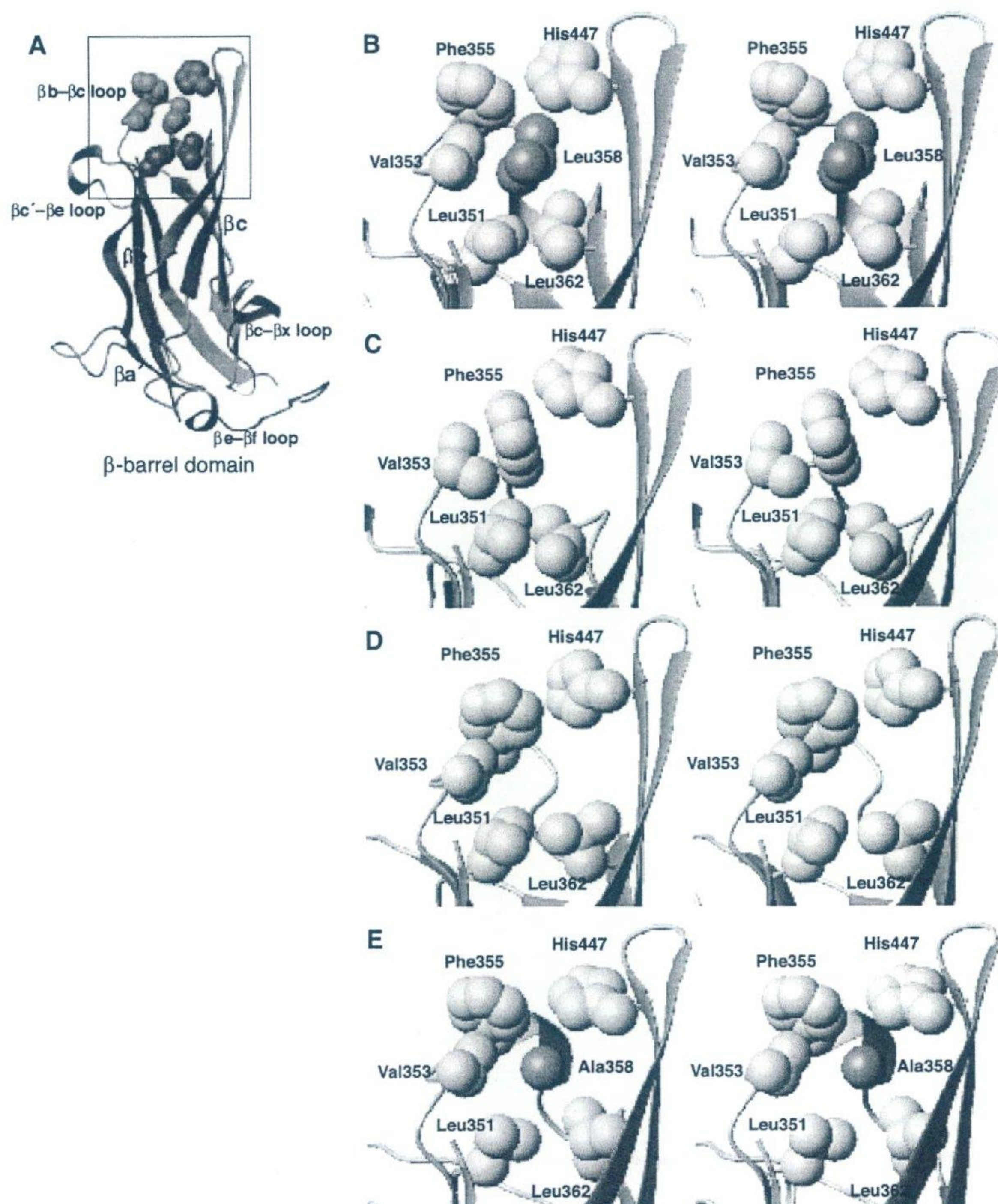

FIG. 9. Structure of the wild-type STAT3 and homology models of the hydrophobic core surrounding Leu358. The crystal structure of the β-barrel domain of the wild-type STAT3β (A) and its hydrophobic core region (B). In panel A, the B-factors are color coded, with lower values in blue and higher values in red, to show that the loop bearing L358 is well-ordered and rigid. (C to E) The hydrophobic core regions of the dD7, dL358, and L358A mutants, respectively. In panels B to E, only the residues corresponding to the boxed region of panel A are shown. The key residue, Leu358, is highlighted in orange, and the surrounding hydrophobic residues that form the core together with Leu358 are shown in yellow. The figures are in stereo view (wall eye) and were produced using MOLMOL (20). It should be noted that all of these modeled core structures are packed less tightly than the wild-type structure.

Downloaded from mcb.asm.org at UNIV OF TOKYO on March 29, 2009

of the βc strand in the β-barrel domain, as shown in Fig. 5A and 9A. The tertiary structure of this domain appears to be rigid, as its B-factors (ca. 51 $Å^2$) are considerably lower than those of the other domains of the protein (ca. 66 $Å^2$). Deletion mutants of the βb strand (dD3 to dD5) resulted in loss of the MgcRacGAP binding ability of STAT3, suggesting that the βb strand is the MgcRacGAP binding site. Interestingly, the MgcRacGAP binding ability and the transcriptional activity of STAT3 were enhanced by deletion of the D6 to D9 region (Fig. 5C). These phenotypes may be explained by the flexibility around the βb strand. Within the β-barrel domain, the DNA-bound βa′-βb loop and the βb-βc loop region are as rigid as the β strands (the B-factors, ca. 40 $Å^2$), while the βc-βx, βc′-βe, and βe-βf loops are much more flexible (Fig. 9A). The rigidity of the βb-βc loop is probably because Leu358 in this loop is involved in the hydrophobic core formation. When a deletion mutation is introduced in the βb-βc loop (dD6-dD9, d356P, d357E, and d358L), the tertiary structure of the domain may be retained but become more flexible, as the hydrophobic core is packed less tightly than the wild type (see Fig. 9B, C, and D for representative structural models). These STAT3 mutants with more flexibility around the βb strand (binding site of MgcRacGAP) could bind more efficiently to MgcRacGAP, leading to their enhanced activation. In the L358A mutant, which behaves similarly to the d358L mutant (data not shown), the hydrophobic core of the domain is also loosened (Fig. 9E). Thus, all of these deletion and point mutations may destabilize the hydrophobic core of the domain around the βb strand (binding site of MgcRacGAP) and therefore seem to increase the binding ability of the βb strand to MgcRacGAP. The dD2 and dD10 mutants also strongly bind to MgcRacGAP, possibly because of the distortion of the domain structure, while hyperactive transcription was not observed, as they lacked the DNA binding activities. The loss of the MgcRacGAP binding ability in the dD1 mutant lacking the C terminus of the βa′ strand may be due to a secondary result of structural distortion of the βa′ strand and the DNA-bound βa′-βb loop. Our current hypothesis is that upon binding with MgcRacGAP, the β-barrel domain of STAT undergoes some conformational change so that the MgcRacGAP binding region (the βb strand) becomes more flexible and more exposed.

MgcRacGAP accompanied by GTP-bound Rac1 functions both as a mediator of the tyrosine phosphorylation of STATs and as an NLS-containing nuclear chaperone of p-STATs during interphase, while MgcRacGAP plays a critical role in cell division. We believe that MgcRacGAP is a molecule which functions in the nucleocytoplasmic transporting system during interphase and in the mitotic apparatus from metaphase to cytokinesis, as is the case with nucleocytoplasmic transporters, including importins and Ran, which are also involved in the formation of the mitotic spindle after the disassembly of the nuclear envelope (7). Although MgcRacGAP is not involved in nuclear translocation of NF-κB, whether it is involved in nuclear transport of other proteins is still open to question.

ACKNOWLEDGMENTS

We thank Toshio Hirano for kindly providing BaF-BO3 mutants and Dovie Wylie for language assistance.

This work was supported by the RIKEN Structural Genomics/Proteomics Initiative, the National Project on Protein Structural and Functional Analyses, the Sumitomo Foundation, and the Ministry of Education, Culture, Sports, Science and Technology of Japan.

REFERENCES

1. **Adam, S. A., R. S. Marr, and L. Gerace.** 1990. Nuclear protein import in permeabilized mammalian cells requires soluble cytoplasmic factors. J. Cell Biol. **111:**807–816.
2. **Becker, S., B. Groner, and C. W. Müller.** 1998. Three-dimensional structure of the Stat3β homodimer bound to DNA. Nature **394:**145–151.
3. **Bromberg, J. F., M. H. Wrzeszczynska, G. Devgan, Y. Zhao, R.G. Pestell, C. Albanese, and J. E. Darnell, Jr.** 1999. The JAK-STAT pathway: summary of initial studies and recent advances. Stat3 as an oncogene. Cell **98:**295–303.
4. **Chook, Y. M., and G. Blobel.** 2001. Karyopherins and nuclear import. Curr. Opin. Struct. Biol. **11:**703–715.
5. **Darnell, J. E., Jr.** 2002. Transcription factors as targets for cancer therapy. Nat. Rev. Cancer **2:**740–749.
6. **Darnell, J. E., Jr.** 1996. The JAK-STAT pathway: summary of initial studies and recent advances. Recent Prog. Horm. Res. **51:**391–403.
7. **Dasso, M.** 2001. Running on Ran nuclear transport and the mitotic spindle. Cell **104:**321–324.
8. **Fagerlund, R., L. Kinnunen, M. Köhler, I. Julkunen, and K. Melén.** 2005. NF-κB is transported into the nucleus by importin α3 and importin α4. J. Biol. Chem. **280:**15942–15951.
9. **Fiser, A., R. K. Do, and A. Sali.** 2000. Modeling of loops in protein structures. Protein Sci. **9:**1753–1773.
10. **Fukada, T., M. Hibi, Y. Yamanaka, M. Takahashi-Tezuka, Y. Fujitani, T. Yamaguchi, K. Nakajima, and T. Hirano.** 1996. Two signals are necessary for cell proliferation induced by a cytokine receptor gp130: involvement of STAT3 in anti-apoptosis. Immunity **5:**449–460.
11. **Gorlich, D., and U. Kutay.** 1999. Transport between the cell nucleus and the cytoplasm. Annu. Rev. Cell Dev. Biol. **15:**607–660.
12. **Hirose, K., T. Kawashima, I. Iwamoto, T. Nosaka, and T. Kitamura.** 2001. MgcRacGAP is involved in cytokinesis through associating with mitotic spindle and midbody. J. Biol. Chem. **276:**5821–5828.
13. **Ihle, J. N.** 1996. Janus kinases in cytokine signalling. Philos. Trans. R. Soc. Lond. B **351:**159–166.
14. **Isshiki, H., S. Akira, O. Tanabe, T. Nakajima, T. Shimamoto, T. Hirano, and T. Kishimoto.** 1990. Constitutive and interleukin-1 (IL-1)-inducible factors interact with the IL-1-responsive element in the IL-6 gene. Mol. Cell. Biol. **10:**2757–2764.
15. **Jaffe, A. B., and A. Hall.** 2005. Rho GTPases: biochemistry and biology. Annu. Rev. Cell Dev. Biol. **21:**247–269.
16. **Jantsch-Plunger, V., P. Gonczy, A. Romano, H. Schnabel, D. Hamill, R. Schnabel, A.A. Hyman, and M. Glotzer.** 2000. CYK-4: a Rho family gtpase activating protein (GAP) required for central spindle formation and cytokinesis. J. Cell Biol. **149:**1391–1404.
17. **Kawashima, T., Y. C. Bao, Y. Nomura, Y. Moon, Y. Tonozuka, Y. Minoshima, T. Hatori, A. Tsuchiya, M. Kiyono, T. Nosaka, H. Nakajima, D.A. Williams, and T. Kitamura.** 2006. Rac1 and a GTPase activating protein MgcRacGAP are required for nuclear translocation of STAT transcription factors. J. Cell Biol. **175:**937–946.
18. **Kawashima, T., K. Hirose, T. Satoh, A. Kaneko, Y. Ikeda, Y. Kaziro, T. Nosaka, and T. Kitamura.** 2000. MgcRacGAP is involved in the control of growth and differentiation of hematopoietic cells. Blood **96:**2116–2124.
19. **Kinoshita, E., E. Kinoshita-Kikuta, K. Takiyama, and T. Koike.** 2006. Phosphate-binding tag, a new tool to visualize phosphorylated proteins. Mol. Cell. Proteomics **5:**749–757.
20. **Koradi, R., M. Billeter, and K. Wüthrich.** 1996. MOLMOL: a program for display and analysis of macromolecular structures. J. Mol. Graph. **14:**51–55.
21. **Kutay, U., E. I. Izaurralde, F.R. Bischoff, I.W. Mattaj, and D. Görlich.** 1997. Dominant-negative mutants of importin-β block multiple pathways of import and export through the nuclear pore complex. EMBO J. **16:**1153–1163.
22. **Lanning, C. C., R. Ruiz-Velasco, and C. L. Williams.** 2003. Novel mechanism of the co-regulation of nuclear transport of SmgGDS and Rac1. J. Biol. Chem. **278:**12495–12506.
23. **Latimer, M., M. K. Ernst, L. L. Dunn, M. Drutskaya, and N. R. Rice.** 1998. The N-terminal domain of IκBα masks the nuclear localization signal(s) of p50 and c-Rel homodimers. Mol. Cell. Biol. **18:**2640–2649.
24. **Lee, B. J., A. E. Cansizoglu, K. E. Süel, T. H. Louis, Z. Zhang, and Y. M. Chook.** 2006. Rules for nuclear localization sequence recognition by karyopherin beta 2. Cell **126:**543–558.
25. **Liu, L., K. M. McBride, and N. C. Reich.** 2005. STAT3 nuclear import is independent of tyrosine phosphorylation and mediated by importin-alpha3. Proc. Natl. Acad. Sci. USA **102:**8150–8155.
26. **Ma, J., and X. Cao.** 2006. Regulation of Stat3 nuclear import by importin α5 and importin α7 via two different functional sequence elements. Cell Signal. **18:**1117–1126.
27. **Marg, A., Y. Shan, T. Meyer, T. Meissner, M. Brandenburg, and U. Vinkemeier.** 2004. Nucleocytoplasmic shuttling by nucleoporins Nup153 and Nup214 and CRM1-dependent nuclear export control the subcellular distribution of latent Stat1. J. Cell Biol. **165:**823–833.
28. **Marti-Renom, M. A., A. Stuart, A. Fiser, R. Sanchez, F. Melo, and A. Sali.**

Downloaded from mcb.asm.org at UNIV OF TOKYO on March 29, 2009

2000. Comparative protein structure modeling of genes and genomes. Annu. Rev. Biophys. Biomol. Struct. **29:**291–325.

29. **Mattaj, I., and L. Englmeier.** 1998. Nucleocytoplasmic transport: the soluble phase. Annu. Rev. Biochem. **67:**265–306.
30. **McBride, K. M., G. Banninger, C. McDonald, and N. C. Reich.** 2002. Regulated nuclear import of the STAT1 transcription factor by direct binding of importin-α. EMBO J. **21:**1754–1763.
31. **Michaelson, D., W. Abidi, D. Guardavaccaro, M. Zhou, I. Ahearn, M. Pagano, and M. R. Philips.** 2008. Rac1 accumulates in the nucleus during the G_2 phase of the cell cycle and promotes cell division. J. Cell Biol. **181:**485–496.
32. **Minoshima, Y., T. Hori, M. Okada, H. Kimura, T. Haraguchi, Y. Hiraoka, Y. C. Bao, T. Kawashima, T. Kitamura, and T. Fukagawa.** 2005. The constitutive centromere component CENP-50 is required for recovery from spindle damage. Mol. Cell. Biol. **25:**10315–10328.
33. **Minoshima, Y., T. Kawashima, K. Hirose, Y. Tonozuka, A. Kawajiri, Y.C. Bao, X. Deng, M. Tatsuka, S. Narumiya, W. S. May, Jr., T. Nosaka, K. Semba, T. Inoue, T. Satoh, M. Inagaki, and T. Kitamura.** 2003. Phosphorylation by Aurora B converts MgcRacGAP to a RhoGAP during cytokinesis. Dev. Cell **4:**549–560.
34. **Mishima, M., S. Kaitna, and M. Glotzer.** 2002. Central spindle assembly and cytokinesis require a kinesin-like protein/RhoGAP complex with microtubule bundling activity. Dev. Cell **2:**41–54.
35. **Miura, M., T. Tamura, and K. Mikoshiba.** 1990. Cell-specific expression of the mouse glial fibrillary acidic protein gene: identification of the cis- and trans-acting promoter elements for astrocyte-specific expression. J. Neurochem. **55:**1180–1188.
36. **Morita, S., T. Kojima, and T. Kitamura.** 2000. Plat-E: an efficient and stable system for transient packaging of retroviruses. Gene Ther. **12:**1063–1066.
37. **Onishi, M., T. Nosaka, K. Misawa, A. L. Mui, D. Gorman, M. McMahon, A. Miyajima, and T. Kitamura.** 1998. Identification and characterization of a constitutively active STAT5 mutant that promotes cell proliferation. Mol. Cell. Biol. **18:**3871–3879.
38. **Peifer, M., S. Berg, and A. B. Reynolds.** 1994. A repeating amino acid motif shared by proteins with diverse cellular roles. Cell **76:**789–791.
39. **Ridley, A. J.** 2006. Rho GTPases and actin dynamics in membrane protrusions and vesicle trafficking. Trends Cell Biol. **16:**522–529.
40. **Saharinen, P., K. Takaluoma, and O. Silvennoinen.** 2000. Regulation of the Jak2 tyrosine kinase by its pseudokinase domain. Mol. Cell. Biol. **20:**3387–3395.
41. **Sali, A., and T. L. Blundell.** 1993. Comparative protein modelling by satisfaction of spatial restraints. J. Mol. Biol. **234:**779–815.
42. **Sekimoto, T., N. Imamoto, K. Nakajima, T. Hirano, and Y. Yoneda.** 1997. Extracellular signal-dependent nuclear import of Stat1 is mediated by nuclear pore-targeting complex formation with NPI-1, but not Rch1. EMBO J. **16:**7067–7077.
43. **Tonozuka, Y., Y. Minoshima, Y. C. Bao, Y. Moon, Y. Tsubono, T. Hatori, H. Nakajima, T. Nosaka, T. Kawashima, and T. Kitamura.** 2004. A GTPase activating protein binds STAT3 and is required for IL-6-induced STAT3 activation and for differentiation of a leukemic cell line. Blood **104:**3550–3557.
44. **Ushijima, R., N. Sakaguchi, A. Kano, A. Maruyama, Y. Miyamoto, T. Sekimoto, Y. Yoneda, K. Ogino, and T. Tachibana.** 2005. Extracellular signal-dependent nuclear import of STAT3 is mediated by various importin alphas. Biochem. Biophys. Res. Commun. **330:**880–886.
45. **Van de Putte, T., A. Zwijsen, O. Lonnoy, V. Rybin, M. Cozijnsen, A. Francis, V. Baekelandt, C. A. Kozak, M. Zerial, and D. Huylebroeck.** 2001. Mice with a homozygous gene trap vector insertion in mgcRacGAP die during pre-implantation development. Mech. Dev. **102:**33–44.
46. **Wang, J. M., P. Cieplak, and P. A. Kollman.** 2000. How well does a restrained electrostatic potential (RESP) model perform in calculating conformational energies of organic and biological molecules? J. Comput. Chem. **21:**1049–1074.
47. **Wu, X. M., X. L. Tu, K. S. Joeng, M. J. Hilton, D. A. Williams, and F. X. Long.** 2008. Rac1 activation controls nuclear localization of beta-catenin during canonical Wnt signaling. Cell **133:**340–353.
48. **Yamada, T., T. Kurosaki, and M. Hikida.** 2008. Essential roles of MgcRacGAP in multilineage differentiation and survival of murine hematopoietic cells. Biochem. Biophys. Res. Commun. **372:**941–946.
49. **Zeng, R., Y. Aoki, M. Yoshida, K. Arai, and S. Watanabe.** 2002. Stat5B shuttles between cytoplasm and nucleus in a cytokine-dependent and -independent manner. J. Immunol. **168:**4567–4575.

Downloaded from mcb.asm.org at UNIV OF TOKYO on March 29, 2009